EVIDENCE OF A QUARK IN A HIGH-ENERGY COSMIC-RAY BUBBLE-CHAMBER PICTURE*

W. T. Chu and Young S. Kim
Physics Department, Ohio State University, Columbus, Ohio 43210

and

W. J. Beam
Physics Department, Rose Polytechnic Institute, Terre Haute, Indiana 47803

and

Nowhan Kwak
Physics Department, University of Kansas, Lawrence, Kansas 66044
(Received 11 February 1970)

We have found a bubble-chamber picture which shows three contemporaneous high-energy cosmic-ray tracks. One of the tracks has ionization which is that expected of a charge-$\frac{2}{3}$ particle if the mass of this particle is less than 6.5 GeV. The observed ionization is also consistent with that which is expected of a charge-$\frac{1}{3}$ particle with a mass of 8.0 ± 3.0 GeV.

Recently, McCusker et al.[1] have reported on five cloud-chamber pictures that show tracks which are less ionizing than would be possible for singly charged particles. The authors state that these tracks were due to "quarks" of charge $\frac{2}{3}$. Several authors[2-4] have claimed that McCusker et al. did not properly consider the effects of the relativistic rise of ionization and the statistical fluctuations in drop-formation processes. However, these claims are being rebutted by McCusker et al.[5] at present.

Motivated by McCusker et al.'s report, we have been looking for high-energy "shower" events which contain one or more "old"-looking tracks in a heavy-liquid bubble chamber. A shower event is required to have at least one "straight" ($P > 100$ GeV/c) track accompanied by several other moderately (about 5 GeV/c or more) high-energy tracks coming into the chamber in similar directions. We wish to point out that heavy-liquid bubble-chamber pictures exposed to low-energy particles at accelerators are usually low-sensitivity (low temperature and large pressure drops) exposures and that they are suitable for quark search in cosmic-ray particle tracks recorded as backgrounds in the pictures. For low-sensitivity exposures, one has a larger rate of bubble growth but a smaller rate of sensitivity variation in time and it is possible to pick out contemporaneous tracks with moderately precise measurements of the relative size of bubbles.[6] For exposures in which beam particles are let into the chamber at the maximum sensitivity, the effective time window during which the chamber is sensitive for "quark" detection is set by diffraction limits on one end (too "young" tracks) and by the retarded bubble growth on the other end (too "old" tracks). Outside these two limits, bubble-image size changes little, whereas the chamber sensitivity may change appreciably and one finds tracks that have the same bubble size but different ionization in many bubble-chamber pictures. We wish to point out that fairly simple quantitative examinations should enable one to determine these two limits for a given exposure. For high-sensitivity exposures, one usually has a rapid change in bubble density but slower bubble growth[6] and the two limits would overlap with each other, making these pictures unsuitable for quark search.

So far we have found one shower event (see Fig. 1) in a sample of 5000 heavy-liquid bubble-chamber pictures (courtesy of Argonne National Laboratory) but none in another sample of 5000 pictures (courtesy of D. Sinclair). The photograph in Fig. 1 shows three contemporaneous and high-energy cosmic-ray tracks. One of these —track C in the figure— has momentum and bubble density which correspond to the ionization expected of either a "quark" of charge $\frac{2}{3}$, if the mass of this "quark" is less than 6.5 GeV, or a "quark" of charge $\frac{1}{3}$, if the mass $= 8.0 \pm 3.0$ GeV.

Table I lists the average of several independent measurements of standard bubble-chamber-track parameters reconstructed in real space. A unit electron charge was assumed for all tracks in computing momentum. In our coordinate system, the $+y$ axis is along the celestial zenith, the $+x$ axis points to the earth's north pole, and the $+z$ axis points to the west. The magnetic field in the chamber was directed along the negative z axis, i.e., into the chamber from

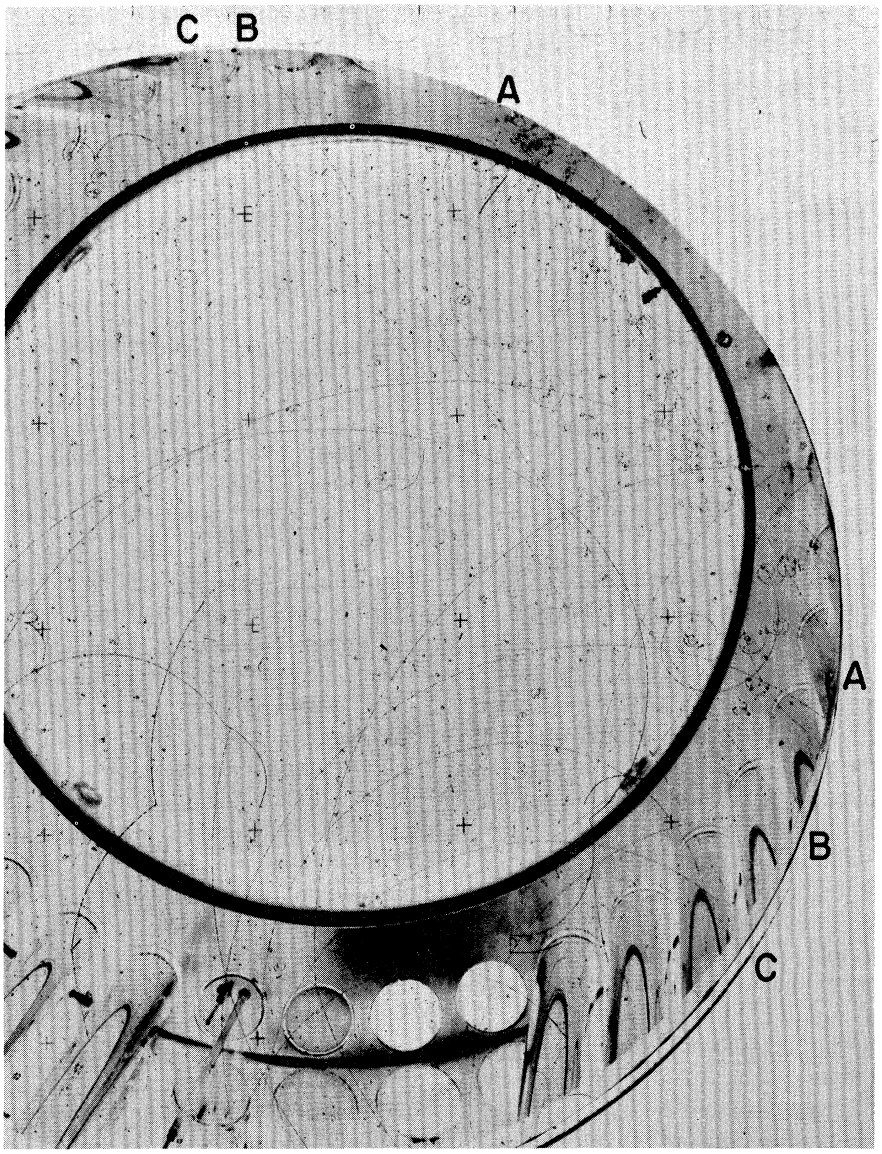

FIG. 1. A heavy-liquid bubble-chamber photograph showing three high-energy and comtemporaneous cosmic-ray tracks. Most *probably*, track A is a hadron coming into the chamber with a large electromagnetic shower and apparently interacted at a point *below* the chamber, shooting up track B (also a hadron) into the chamber. Track B has interacted in the liquid and shows a stopping track pointing skywards. Track C does not appear to meet with any of the other cosmic-ray tracks but can be shown to be contemporaneous with them from bubble-diameter measurements. We believe track C is due to a fractionally charged particle.

the camera end. The dip and azimuth have the usual meaning but the zenith is the angle tracks made with the celestial zenith. The relative space angles among the three tracks are 7.3°, 19.4°, and 12.1° between tracks A and B, between tracks A and C, and between tracks B and C, respectively. These angles were computed from the incident direction of the tracks at the top of the chamber view.

The bubble chamber [University of Michigan–Argonne 40-in. heavy-liquid bubble chamber (HLBC)] was shielded with steel (60-cm-thick) and copper (80-cm-thick) enclosures. This gives a minimum path length of about 95 radiation lengths or about 1200 g/cm^2, corresponding to about 2 GeV energy loss by medium-energy (about 10-GeV) muons. In Fig. 1 it can be seen that track A is accompanied by some 60 electrons visible in the chamber and that track B has interacted in the liquid showing a short stop-

Table I. Track parameters in real space.

Track	Momentum (GeV/c)	Length (cm)	Dip (deg)	Azimuth (deg)	Zenith (deg)	Average over four views Number of bubbles	Bubble density
A	$\pm 600^{+\infty}_{-400}$ [a]	55.7[b]	−7.7	120.2	31.2[c]		
B	$+8.8 \pm 0.2$[d]	78.7	−0.35	120.2	30.2	364	4.56 ± 0.30[e]
C	-8.7 ± 0.2[d]	72.5	11.64	122.2	34.0	167	2.17 ± 0.20

[a] A unit charge and downward (normal cosmic ray) directions were assumed in computing momentum.
[b] Since not all visible lengths could be measured, these lengths are slightly less than the total visible lengths.
[c] This is the celestial zenith angle.
[d] These two momenta correspond to about 11 GeV/c at sea level due to the energy loss in the magnet iron and copper coils surrounding the chamber.
[e] Bubble density in real space given in units of bubbles/cm.

ping track (B also shows two low-energy delta rays). The stopping track is presumably a proton from its appearance and points skywards, suggesting, but not necessarily proving, that track B is an "albedo." Indeed, it can be shown that A and B intersect within 20-30 mm in space beneath the chamber magnet.[7] Since the muon-nucleon interaction cross section is some 3 to 4 orders of magnitude less than the hadron interaction cross section, it is highly improbable that B is a muon. The fact that B is passing through the beam port certainly helps the thesis that it is a hadron albedo. As shown later, the observed bubble density of B clearly shows that it is a singly charged particle. In this paper, we will consider two possibilities: (a) B is a 1.3-times-minimum ionizing particle (muon or pion) and (b) B is a 1.08-times-minimum ionizing particle (proton or antiproton).

Track C does not appear to meet with either of the two tracks. But unlike track B, C passes through some material near ground and may have easily suffered "strong force" deflections. A deflection of less than 8° would make C intersect with the A-B intersection point; or a deflection of less than 3° would make B and C meet in space.

For the purpose of bubble-density comparison, we note that A is in the ultrahigh-energy region where bubble density and dE/dx are not simply related and so only B can be safely used as the "comparison" track. Since the chamber sensitivity was not constant in time, it is essential for us to establish the contemporaneity of B and C. Had B and C met in space, their contemporaneity would have been established with near certainty. We establish the contemporaneity of B and C from their bubble diameter distribution.

The bubble size and bubble separation of tracks A, B, and C, as well as some forty cosmic-ray muon tracks (with energy greater than 10 GeV) and several hundred beam tracks in the roll, were measured on a 50× traveling microscope by one and the same measurer.[8] Periodic random measurements showed that the average bubble size and bubble separation were reproducible within ±2 microns on film. Due to the particular mode of 90° illumination used in the chamber (i.e., 30 flash tubes "embedded" in the walls of the liquid cylinder), considerable variations in the amount of light scattered into a camera by a bubble were expected and were indeed found. It was observed that the size of bubble images of tracks dipping into the chamber from the front window and cutting into the back flange varied by as much as a factor of three, being largest near the window. This factor is what one would expect from Welford's formulas[9] for the 40-in. optics. We have written a computer program which takes Welford's formulas and integrates over the light sources. This program computes the relative flux of light scattered by a unit-radius bubble into a camera through various refractive media as function of the bubble location in the chamber. We found that an empirical equation, $d = Ar/G + BrI_0^{1/2}$ (d is the bubble-image diameter, r is the real bubble radius, G is the geometric demagnification factor, and I_0 is Welford's formula per unit radius), describes very well the observed variations of bubble images along tracks. Of course, it is impossible to determine the absolute value of r from our expression above but it should be noted that we are interested only in the relative bubble size and the quantity "relative bubble diameter," $D = 0.1d/(G^{-1} + qI_0^{1/2})$, is of relevance to us. I_0 was normalized to unity at the center of the chamber and the empirical constant q was about 0.1 for all tracks considered in the roll. The geometrical demagnification factor G was 16.25 at the front

window ($z = 0.0$) and it was 21.3 at the flange ($z = -64.89$ cm). The observed bubble-image diameters varied from about 12 to over 60 μm on film. The diameter of the first Airy disc was computed to be about 14 μm for the chamber optics.

The bubble separation was corrected for each view for dip and demagnification and the most probable bubble density was then obtained by the maximum-likelihood method of Barkas.[10] Table I gives the observed bubble density of tracks B and C. In two of the four independent views studied, some portions of these tracks appeared faint as a result of poor illumination. However, the bubble density measured with the faint portions left out did not differ much from the overall bubble density.

A reliable estimate of the dependence of bubble density on the track age for a given dE/dx can be made from the recorded time variation of the dynamic liquid pressure and a certain kind of information on the 40-in.-HLBC characteristics. Figure 2(a) gives the pressure drop (the vapor equilibrium pressure at 40°C minus the dynamic liquid pressure) as a function of track age. For the "quark" frame, the average bubble diameter of beam tracks was 18.5 ± 1.0 μm on film (about 20 in our relative bubble-diameter scale) and the average bubble density (700-MeV/c K^+ at entrance) was 7.5 ± 0.8 bubbles/cm in real space. From the well-known fact that for small t (track age in milliseconds) bubble diameter is very accurately given by the $t^{1/2}$ rule, and from the known age of beam tracks (6 msec), one may establish the time scale for our tracks as shown in Fig. 2(b) (curve I). It is also well known that[11,12] old bubbles do not follow the $t^{1/2}$ rule and we estimate that a more realistic time scale is given by curve II in Fig. 2(b) (our basic conclusions are not sensitive to which curve one takes and, for simplicity, we consider only II in the following discussions). The small open circles along curve II in Fig. 2(b) represent cosmic-ray muon tracks found in the "quark" roll. These muons had energy greater than 10 GeV and they were part of a previous study of cosmic-ray muon intensity.[13] Tracks younger than the beam tracks are near or at the diffraction limits and they are found, usually, near the front window (in the back region of the chamber, the light flux scattered back into the camera is small and only relatively large bubbles are photographed from this region). On the other hand, very old tracks generally show large rms track-fit errors[13] due, presumably, to liquid motion, bubble ascension, etc. and are more likely to be rejected in the recon-

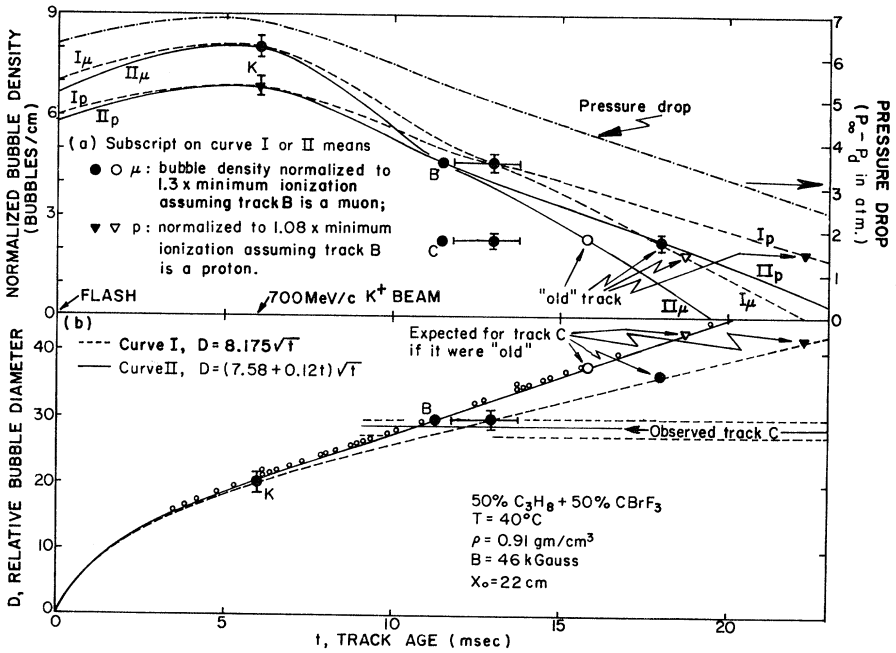

FIG. 2. (a) Bubble chamber "sensitivity" curves as function of track "age." The pressure drop is the vapor equilibrium pressure at 40°C minus the dynamic liquid pressure. The two curves of bubble density versus track age were computed from the beam-track bubble density and the track-B bubble density for two possible values of mass for track B. (b) Relative bubble diameter (in an arbitrary scale) as function of track age. The small open circles along curve II represent cosmic-ray muons with energy greater than 10 GeV found in the roll.

struction program than are younger tracks. In addition, since there is about one random-noise bubble per cm^2 (projection on scan tables), older tracks—and very lightly ionizing tracks—are harder to detect than "normal" tracks. Therefore, it is expected that track-detection efficiency should decrease with track age. When one takes these into account, our derived time scale is in good accordance with an estimate of the "effective" sensitive time of the 40-in. HLBC (8-10 msec) obtained by normalizing the number of muons found in about 50 rolls (including the "quark" roll) to the counter data.[13,14] The number of muons found in our roll did not differ much from the average number of muons per roll in the sample.

Figure 2(a) shows a set of bubble-density versus track-age curves obtained from the "superheat" curve [also shown in Fig. 2(a)] and the two known points on the curve (beam tracks and track B). Curve II_μ was generated for $dE/dx = 1.3(dE/dx)_{min}$—i.e., track B is assumed to be a muon or a pion.[15] The observed bubble density of track C on this curve would put its age at about 16 msec if C were an old muon. A muon track at this age on curve II in Fig. 2(b) would have a relative bubble diameter which is some six standard deviations (about five standard deviations on curve I) larger than the observed value. Curve II_p was generated for $dE/dx = 1.08(dE/dx)_{min}$—i.e., track B is assumed to be a proton. It is seen that on this curve track C would be about 18.8 msec old if it were an old muon. This age corresponds to a diameter which is nine standard deviations larger than the measured value. Figure 3 shows bubble density versus the relative bubble diameter for all muons with energy greater than 10 GeV found in the roll, for comparison with our curves in Fig. 2. It should be noted that the large spread of points is due to variations in pressure patterns in the 40-in. chamber. The chamber was not pressure stabilized and considerable fluctuations in pressure-drop patterns could be observed (for example, the bubble density of beam tracks varied by as much as 30% from frame to frame in the roll). It is precisely because of this kind of fluctuation in bubble-chamber operations (at least those bubble chambers which are not "stabilized") that one should require the presence of a "comparison" track which is not only contemporaneous with the "quark" candidate but also desirably found in the neighborhood of the candidate in the chamber.

Several tracks found near the region where track C was located had bubble diameter comparable with that of track C but had normal bubble density. Furthermore, the observed bubble density of track C did not vary much over its depth range (the depth of C ranged from $z = -5$ to $z = -20$ cm, as compared with the depth of B which ranged from $z = -32.62$ to -32.00 cm). These rule out the possibility of some local pressure and temperature inhomogeneity which might have caused smaller (as much as 50%) bubble density in track C.

It should be noted that the probability of observing a cosmic-ray muon with E greater than 8 GeV coming into the chamber within a given time interval (say 5 msec) and in a solid angle of $20° \times 20°$ and in an area of 40×40 cm^2 is about one in a thousand (0.001). Therefore, in order that C be an old muon, it must have come into the chamber with a chance of 0.001 and at the same time given an average bubble diameter which is some 6 to 9 standard deviations too small. Or it may be stated that in order that C be a muon (or any of the

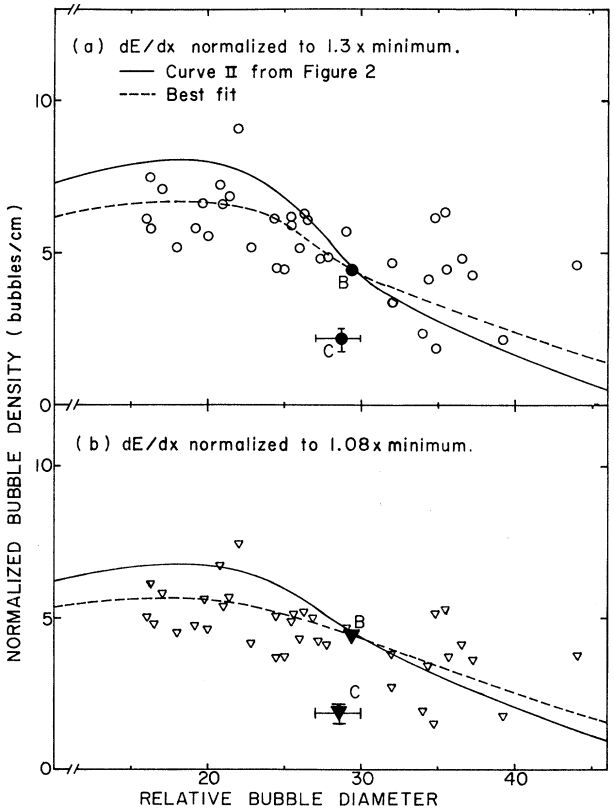

FIG. 3. Bubble density versus relative bubble-diameter correlation as computed from curves given in Fig. 2. The apparent spreads of the experimental points (open circles and triangles) are due to the fact that they came from pressure patterns which were different from that which has produced the "quark" picture.

standard singly charged particles), it must have come in very nearly contemporaneously with B (may even have been coherent with B) but had a bubble density that is some 8 to 10 standard deviations too small. We believe that these two cases (or any combination of the two) are both highly improbable. The presence of track A (which can be shown to be contemporaneous with B from bubble-size measurements) is not necessary for our considerations but a priori its extremely high energy (nominally 600 GeV) makes our claims more plausible in view of the widely held suspicion that if "quarks" really existed, they would be produced at "very" large primary energies.

Figure 4 shows dE/dx for various known singly charged particles as a function of particle momentum.[15] It also shows dE/dx for $\frac{2}{3}$-charge particles with various assumed mass values. In the figure, we show two possible situations: (a) B is a muon or a pion and (b) B is a proton (antiproton). In both cases, it is clear that an upper limit on the mass of a $\frac{2}{3}$-charge "quark" may be placed at about 6.5 GeV with better than 90% confidence. No significant estimate on a lower limit of the mass can be made from our data. Our data are also consistent with a $\frac{1}{3}$-charge "quark" if the mass of this particle is 8.0 ± 3.0 GeV.

In summary, we have observed three contemporaneous and high-energy tracks (A, B, and C in Fig. 1) in a bubble-chamber picture. A and B appear to meet at a point underground; track C, even though it does not appear to meet with A or B, can be shown to be contemporaneous with A and B from bubble-diameter measurements. Track C has an apparent momentum which is nearly identical to that of track B but it has bubble density which is less than $\frac{1}{2}$ of that of track B. We have shown that this low bubble density can not be explained in terms of any currently known phenomenon and that it is consistent with being the result of a fractionally charged particle such as the legendary "quarks."

We wish to thank Professor H. J. Martin and Professor J. Mott for enabling us to make an independent measurement of some of the basic numbers in our data. We wish to thank Professor D. Sinclair, Professor C. Nielsen, Professor K. Tanaka, Professor W. Mitchell, and Dr. R. Walker for many technical assistances and helpful discussions. We wish to thank Miss K. Schonmeyer for scanning and measuring the film so reliably and enthusiastically. We wish to thank Mr. V. Sevcik and his crew of the 40-in. chamber for the most willing and useful cooperation and services. We wish to thank Dr. B. Cork and Professor A. Wolfendale for pointing out several critical flaws in a preliminary version of this paper. One of us (Y.S.K.) wishes to thank Professor E. L. Jossem for his financial and moral support of this work.

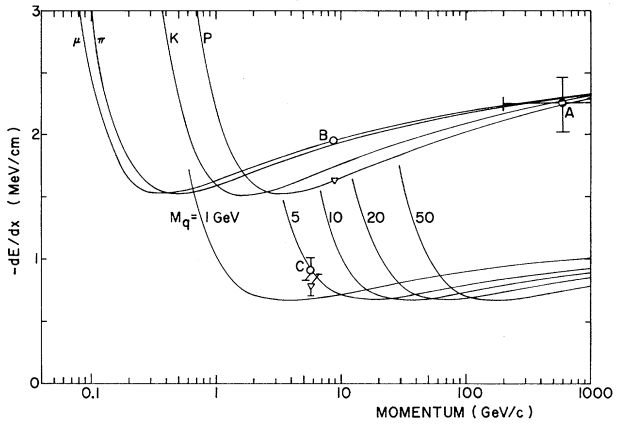

FIG. 4. Energy loss per unit length versus particle momentum for some known singly charged particles and for particles of charge $\frac{2}{3}$, assuming various mass values. Circles correspond to the assumption that B is a muon or a pion, and triangles correspond to the assumption that B is a proton (an antiproton if B is an albedo).

*Work supported in part by the U. S. Atomic Energy Commission.

[1]C. B. A. McCusker and I. Cairns, Phys. Rev. Letters 23, 658 (1969); I. Cairns, C. B. A. McCusker, L. S. Peak, and R. L. S. Woolcott, Phys. Rev. 186, 1394 (1969).

[2]H. Frauenfelder, U. E. Kruse, and R. D. Sard, Phys. Rev. Letters 24, 33 (1970).

[3]R. K. Adair and H. Kasha, Phys. Rev. Letters 23, 1355 (1969).

[4]D. C. Rahm and R. I. Louttit, Phys. Rev. Letters 24, 279 (1970).

[5]C. B. A. McCusker, private communications.

[6]P. Kunkel, "Erzeugung und Wachsen von Blasen im Arbeitsbereich einer druckstabilisierten Propan-Blasenkammer," Würzburg, 1967 (unpublished).

[7]We wish to thank Mr. R. Larry for computing the fields in the magnet coil and iron for us.

[8]We wish to thank the Astronomy Department at Ohio State University for letting us use its measuring devices.

[9]W. T. Welford, in *Bubble and Spark Chambers*, edited by R. P. Shutt (Academic, New York, 1967), Vol. 1, p. 233.

[10]W. H. Barkas, Phys. Rev. 124, 897 (1961).

[11]S. Wolff, DESY Report No. B1-1, 1969 (unpublished).

[12]Yu. Alexandrov, G. S. Voronov, V. M. Gorbunkov, N. B. Delone, and Yu. I. Nechayev, *Bubble Chambers* (Indiana Univ., Bloomington, Ind., 1967).
[13]Y. S. Kim and L. Voyvodic, to be published.
[14]See for example, M. G. K. Menon and P. V. Ramana Murthy, *Progress in Elementary Particles and Cosmic Ray Physics* (Wiley, New York, 1967), Vol. 9, p. 217.
[15]We have computed dE/dx for our freon-propane mixture using data given by R. M. Sternheimer in Phys. Rev. 145, 247 (1966).

FREQUENCY OF PULSAR STARQUAKES*

R. Smoluchowski
Princeton University, Princeton, New Jersey 08540
(Received 13 March 1970)

A relationship between the frequency of the occurrence of starquakes on pulsars and the shear strength of the solid crust of these objects is derived assuming various mechanisms of damping of their rates of rotation. Tentative conclusions concerning the shear strength, the age, and the composition of the Crab and the Vela pulsars are made.

Several models[1-4] have been proposed to explain the sudden increases in 1969 in frequency[5-8] of pulsars NP0532 (Crab) and PSR0833 (Vela). In this note only Ruderman's model, in which it is assumed that the spinup is a result of a sudden adjustment of the shape of the solid crust of the star, i.e., a starquake, will be discussed. These periodic adjustments relieve strains which build up in the crust as the pulsar's angular velocity slowly decreases. There are two (approximate) equations[2] which govern these phenomena:

$$\varphi \simeq (7R^3/8GM)(\omega_i^2-\omega^2)\sin^2\theta, \tag{1}$$

$$\frac{\Delta R}{R} \simeq \frac{95\mu\varphi_m R}{7GM\rho}\left[1-\left(\frac{R_i}{R}\right)^7\right](1-3\cos^2\theta), \tag{2}$$

in which R and M are the radius and mass of the pulsar, R_i is the inner radius of the crust, G is gravitational constant, φ is the angular shearing strain on the surface of the crust produced when the initial angular velocity ω_i gradually drops to ω, μ is the shear modulus, φ_m is the maximum elastic shear angle, and θ is the latitude measured from the equator. For the Crab and Vela pulsars, the best estimated values for R are 14.6 and 17.4 km, those for M are $0.30M_\odot$ and $0.21M_\odot$ where $M_\odot$ is solar mass; the central densities are $(3.2 \text{ and } 2.45)\times 10^{14}$ g cm^{-3}, and the present angular velocities are 190 and 70 sec^{-1}, respectively. These values are obtained from a variety of considerations[9,10] and the Cameron-Tsuruta[11] equation of state. The inner radius for the Vela[9] pulsar is $R_i = 8.4$ km; for the Crab pulsar this radius is unknown but one expects it to be much smaller. The shear modulus of a Coulomb lattice, i.e., nuclei of charge Z embedded in a relativistic degenerate electron Fermi sea, can be obtained[12] from the approximate relationship $\mu \sim (Ze)^2 m^{4/3}$, where m is the numerical density of nuclei, giving[2] (for Z between 30 and 50) $\mu = 10^{30}$ dyn cm^{-2}. As the angular velocity of the pulsar drops, the surface strains build up, according to Eq. (1), until they reach φ_m. Then, according to Eq. (2), a sudden change of shape occurs which leads to an increase in angular velocity given by $\Delta\omega/\omega = 2\Delta R/R$ for $\theta = \frac{1}{2}\pi$. The observed $\Delta\omega/\omega$ indicate that only a very small fraction of the total surface strain φ_m is removed suddenly during the quake, which suggests that the rest of the strain is relieved gradually through plastic deformation of the solid crust. Such deformation is known to account very well for the continental drift on Earth which is of the order of a few cm per year. This gradual relief of strain will affect the $\omega(t)$ curve[13] and superimpose on the effect of the various damping mechanisms between the core and the crust.[14] It will be assumed here that the gradual relief of the total long-range strain does not affect the interval τ between quakes.

Clearly, the least certain quantity in the above equations is φ_m. Simple theoretical calculations[15] based on chemically and crystallographically perfect crystals of "terrestrial" metals lead to values between 10^{-1} and 10^{-2}. Unfortunately, φ_m is a "structurally sensitive" quantity and, in contrast to the shear modulus μ, its value is radically changed by going from an ideal crystal to a real polycrystal which has chemical impurities, lattice defects, etc. One would expect the pulsar crust to be "impure" in the sense that there may be a whole range of Z values rather than just one, as a result of partial burning and incomplete mixing[16,17], and one would also expect it to contain a host of defects such as grain boundaries, dislocations, etc., produced during

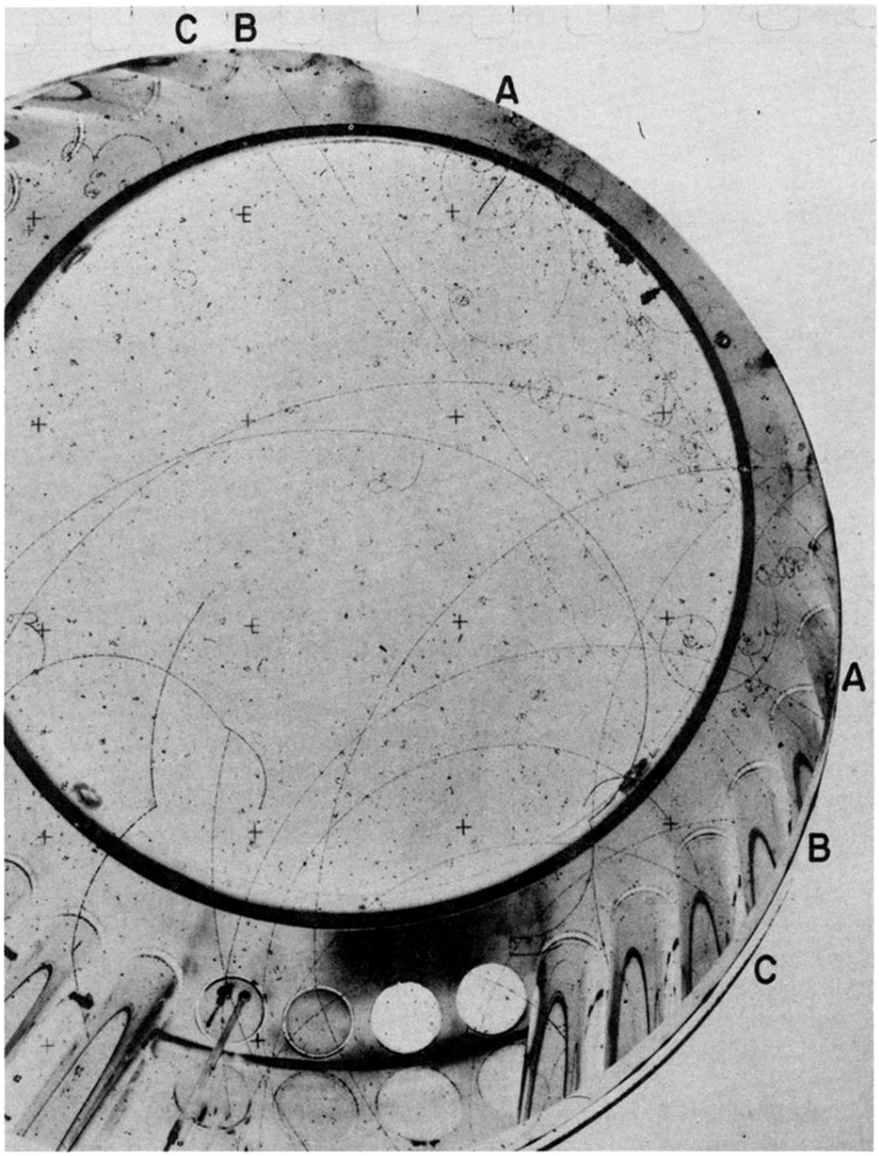

FIG. 1. A heavy-liquid bubble-chamber photograph showing three high-energy and comtemporaneous cosmic-ray tracks. Most *probably*, track *A* is a hadron coming into the chamber with a large electromagnetic shower and apparently interacted at a point *below* the chamber, shooting up track *B* (also a hadron) into the chamber. Track *B* has interacted in the liquid and shows a stopping track pointing skywards. Track *C* does not appear to meet with any of the other cosmic-ray tracks but can be shown to be contemporaneous with them from bubble-diameter measurements. We believe track *C* is due to a fractionally charged particle.